Fish and Shellfish Immunology 93 (2019) 841–850

Contents lists available at ScienceDirect

Fish and Shellfish Immunology

journal homepage: www.elsevier.com/locate/fsi

Full length article

A bactericidal permeability-increasing protein (BPI) from manila clam *Ruditapes philippinarum*: Investigation on the antibacterial activities and antibacterial action mode

Dinglong Yang[a,b], Yijing Han[a,d], Lizhu Chen[e], Ruiwen Cao[a,d], Qing Wang[a,b], Zhijun Dong[a,b], Hui Liu[a,b], Xiaoli Zhang[a,b], Qianqian Zhang[a,b], Jianmin Zhao[a,b,c,*]

[a] Muping Coastal Environment Research Station, Yantai Institute of Coastal Zone Research, Chinese Academy of Sciences, Yantai, 264003, PR China
[b] Research and Development Center for Efficient Utilization of Coastal Bioresources, Yantai Institute of Coastal Zone Research, Chinese Academy of Sciences, Yantai, 264003, PR China
[c] Center for Ocean Mega-science, Chinese Academy of Sciences, Qingdao, 266071, PR China
[d] University of Chinese Academy of Sciences, Beijing, 100049, PR China
[e] Shandong Marine Resource and Environment Research Institute, Yantai, 264006, PR China

ARTICLE INFO

Keywords:
Ruditapes philippinarum
Bactericidal permeability-increasing protein
Antimicrobial activity
Membrane disruption

ABSTRACT

Bactericidal permeability-increasing protein (BPI) is an antimicrobial protein with potent endotoxin-neutralising activity and plays a crucial role in innate immunity against bacterial infection. In the present study, a *bpi* (designed as *rpbpi*) was identified and characterized from manila clam *Ruditapes philippinarum*. Multiple alignments and phylogenetic analysis suggested that *rpbpi* was a new member of the *bpis* family. In non-stimulated clams, *rpbpi* transcripts were ubiquitously expressed in all tested tissues with the highest expression level in hemocytes. After *Vibrio anguillarum* challenge, the expression levels of *rpbpi* mRNA in hemocytes were up-regulated significantly at 3 h and 48 h compared with that in the control, which were 4.01- and 19.10-fold ($P < 0.05$), respectively. The recombinant RpBPI (rRpBPI) showed high antibacterial activities against Gram-negative bacteria *Escherichia coli* and *V. anguillarum*, but not *Staphylococcus aureus*. Moreover, membrane integrity analysis revealed that rRpBPI increased the membrane permeability of Gram-negative bacteria, and then resulted in cell death. Overall, our results suggested that RpBPI played an important role in the elimination of invaded bacteria through membrane-disruptive activity.

1. Introduction

The innate immune system constitutes the first line of host defense. Many of the immune molecules have been found to interact with and respond to the bacterial surface specifically. Two of these proteins, LPS-binding protein (LBP) and bactericidal permeability-increasing protein (BPI) are crucial to the mediation of signals for lipopolysaccharide (LPS) [1]. They shared high similarity and showed high binding ability to Lipid A, a component of LPS [2,3]. Even though these two proteins have similar structures, some biological roles of LBP and BPI are different. For example, LBP usually binds to LPS and significantly facilitates the process of LPS presentation to $CD14^+$ cells, such as macrophages and monocytes [4], while BPI suppresses LPS bioactivity and diminishes it [5,6].

BPI is a cationic antimicrobial polypeptide detected in neutrophil of vertebrates initially [7]. The structure and functions of the protein have been well studied in mammals. They share two common domains: an N-terminal BPI/LBP/CETP domain BPI1 and a C-terminal BPI/LBP/CETP domain BPI2. In general, this protein is usually expressed, to a lesser extent, in monocytes, eosinophils, fibroblasts and epithelial cells [5–8]. Mammal BPI showed high affinity for the lipid A region common to all LPS of Gram-negative bacteria [7]. The direct interaction contributes to its antibacterial activities, such as performing antimicrobial activity directly, binding LPS thereby neutralising endotoxic activity and performing opsonic activity [9]. In mollusk, only a few *bpis* have been identified, and their *bpi* transcripts are also expressed in the immune-related tissues (e.g. gills and digestive glands), and exhibit obvious immune responses against invading bacteria, especially Gram-negative bacteria [10,11].

The manila clam *Ruditapes philippinarum* is one of the most

* Corresponding author. Muping Coastal Environment Research Station, Yantai Institute of Coastal Zone Research, Chinese Academy of Sciences, Yantai, 264003, PR China.
E-mail address: jmzhao@yic.ac.cn (J. Zhao).

https://doi.org/10.1016/j.fsi.2019.08.050
Received 29 March 2019; Received in revised form 15 August 2019; Accepted 16 August 2019
Available online 17 August 2019

commercially important bivalves worldwide. Recent mass mortalities in manila clams have been attributed to pathogen invasion and environmental deterioration [12]. Therefore, it is urgently needed to characterize the immune-related molecules for the disease control and healthy management of clam aquaculture. Presently, several *bpis* have been identified in invertebrates, such as *Apostichopus japonicas* [13], *Crassostrea gigas* [11] and *Biomphalaria glabrata* [14]. The recombinant Cg-BPI2 from oyster *C. gigas* harbored binding activity towards LPS and possessed antibacterial activities against Gram-negative bacteria *Escherichia coli* and *Vibrio alginolyticus* [11]. However, the knowledge on the function of BPI in clams is still limited. In the study, a *bpi* (designated as *rpbpi*) was identified from manila clam *R. philippinarum*, and the spatiotemporal expression profiles, bactericidal activities as well as antibacterial action were also investigated to provide evidence for better understanding the immune responses of clams against pathogens.

2. Materials and methods

2.1. Clams and bacterial challenge

The clams *R. philippinarum* (shell length: 3.0–4.0 cm) were purchased from a local farm and acclimated at 20–22 °C and 30‰ salinity for one week before processing. The clams were fed with an algae mixture of *Isochrysis galbana* and *Phaeodactylum tricornutum*, and the seawater was totally renewed every day. The clams were randomly divided into six tanks with 50-L capacity, each containing 100 clams. Three tanks served as the control, while the other three tanks were immersed with high density of *V. anguillarum* with a final concentration of 1×10^7 CFU mL^{-1}. Hemolymphs of 6 individuals for each treatment were randomly sampled at 0, 6, 12, 24, 48 and 72 h post bacterial challenge. Meanwhile, five tissues, including hemocytes, mantle, gills, hepatopancreas and adductor muscle from 6 individuals of the control group, were collected to investigate the tissue-specific expression of *rpbpi* transcripts.

2.2. RNA extraction and cDNA synthesis

Total RNA was extracted from hemocytes, mantle, gills, hepatopancreas and adductor muscle using TRIzol reagent (Invitrogen). The quality and concentration of total RNA were estimated using a NanoDrop 2000 Spectrophotometer (Thermo Fisher Scientific, USA). Total RNA was treated with RQ1 RNase-Free DNase (Promega, USA) to remove DNA contamination. To synthesize cDNA by reverse transcription, 2 μg total RNA, 200 units M-MLV reverse transcriptase (Promega, USA) and 0.5 μM oligo (d_T) primer were reacted for 1 h at 42 °C in 25 μL reaction mixture.

2.3. Gene cloning of rpbpi

A sequence highly homologous to *bpi* was identified through large scale EST sequencing of the cDNA library constructed from manila clam [15]. Nested-PCR was performed with P1, P2 as forward primers (Table 1) and oligo (d_T) as reverse primer to amplify the 3' end of *rpbpi*. The procedure was listed as follows: the first cycle included an extended (5 min) denaturation period during which polymerase was added (hot-start PCR); 35 cycles of 94 °C for 50 s, 60 °C for 30s and 72 °C for 30 s; the last cycle had an extended elongation period of 72 °C for 10 min. The PCR products were gel-purified, cloned into the pMD19-T simple vector (TaKaRa, Japan) and sequenced in both directions with primers M13-47 and M13-RV (Table 1). The full-length cDNA of *rpbpi* was obtained by overlapping the original EST sequence and the amplified fragments.

Table 1
Primers used in the present study.

Primer	Sequence (5′-3′)	Sequence information
P1	TGCCAGTGGTGGTGTTACTCTT	3′ RACE primer
P2	CAGCCCTTCAACAGAGTACGAG	3′ RACE primer
P3	CCTAATTCCTCAGATAGGGAAGCAC	Real-time PCR
P4	TAAGAGTAACACCACCACTGGCAAC	Real-time PCR
P5	CGCACTTCCTCACGCCATCAT	β-actin primer
P6	GCAGCCGTCTCCATTTCTTGTTC	β-actin primer
P7	GGATCCGCTCGAAACCCGGGCTTTAAGGCA	Recombinant primer
P8	CTCGAGTTAATGCCTGATAAATGGCTTG	Recombinant primer
oligo (d_T)	GGCCACGCGTCGACTAGTACT$_{17}$	Adaptor primer
M13-47	CGCCAGGGTTTTCCCAGTCACGAC	Sequencing primer
M13-RV	GAGCGGATAACAATTTCACACAGG	Sequencing primer

2.4. Bioinformatics analysis

The nucleotide sequence was analyzed using the BLAST algorithm, and the deduced amino acid sequence was analyzed with the Expert Protein Analysis System. The protein domains were predicted with the simple modular architecture research tool version 4.0 [16]. Multiple alignments were performed with the ClustalW Multiple Alignment program and Multiple Alignment Show program. A neighbor-joining phylogenetic tree was constructed by MEGA 4.1 with 1000 bootstrap replicates.

2.5. The spatial and temporal expression patterns of rpbpi mRNA

The spatial and temporal expression profiles of *rpbpi* transcripts were assayed in an Applied Biosystem 7500 fast Real-time PCR System. Gene-specific primers (P3 and P4, Table 1) and β-actin primers (P5 and P6, Table 1) were used to amplify the *rpbpi* and internal control fragment, respectively. The cycling protocol was 1 cycle of 94 °C for 5 min; 40 cycles of 94 °C for 50 s, 60 °C for 60 s and 72 °C for 50 s followed by 1 cycle of 72 °C for 10 min. The purity of amplification products was evaluated by dissociation curve analysis. The $2^{-\triangle\triangle CT}$ method was used to analyze the relative expression level of *rpbpi* [17]. All data were given in terms of relative mRNA expressed as mean ± S.D. (N = 6). Statistical analysis was performed by one-way analysis of variance (one-way ANOVA) followed by a Duncan test using SPSS 16.0 software, and *P* values less than 0.05 were considered statistically significant.

2.6. Recombinant expression and purification of recombinant RpBPI

The cDNA fragment encoding mature peptide of *rpbpi* was amplified with gene-specific primers P7 and P8 with *Bam*H I and *Xho* I sites at their 5′ end, respectively (Table 1). After digestion with the restriction enzymes *Bam*H I and *Xho* I, the fragment was then cloned into the expression vector pET-30a (+) (Novagen, USA). The recombinant plasmid pET-30a-RpBPI was verified by sequencing and transformed into *E. coli* BL21 (DE3) (Novagen, USA). Positive transformants were incubated in Luria-Bertani medium containing 50 μg/ml kanamycin. When the cells grew to OD_{600} of 0.5, recombinant RpBPI (rRpBPI) was induced with the addition of isopropyl β-D-1-thiogalactopyranoside (IPTG, Sigma, USA) at the final concentration of 1 mM. rRpBPI with a His-tag at N terminus was purified by Ni^{2+} chelating sepharose column, and refolded in gradient urea-TBS glycerol buffer (50 mmol L^{-1} Tris–HCl, 50 mmol L^{-1} NaCl, 10% glycerol, 2 mmol L^{-1} reduced glutathione, 0.2 mmol L^{-1} oxide glutathione, a gradient urea concentration of 6, 5, 4, 3, 2, 1, and 0 mol L^{-1}, pH 8.0) at 4 °C for 12 h in each gradient [18]. Expression of the rRpBPI was examined by 15% SDS-polyacrylamide gel electrophoresis (SDS-PAGE) and visualized with Coomassie brilliant blue R-250. The concentration of rRpBPI was measured by BCA Protein Assay Kit (Beyotime, China).

2.7. Preparation of antibody

6-week-old mice were immunized with rRpBPI to prepare polyclonal antibody. The mice were intraperitoneally injected with 100 μg

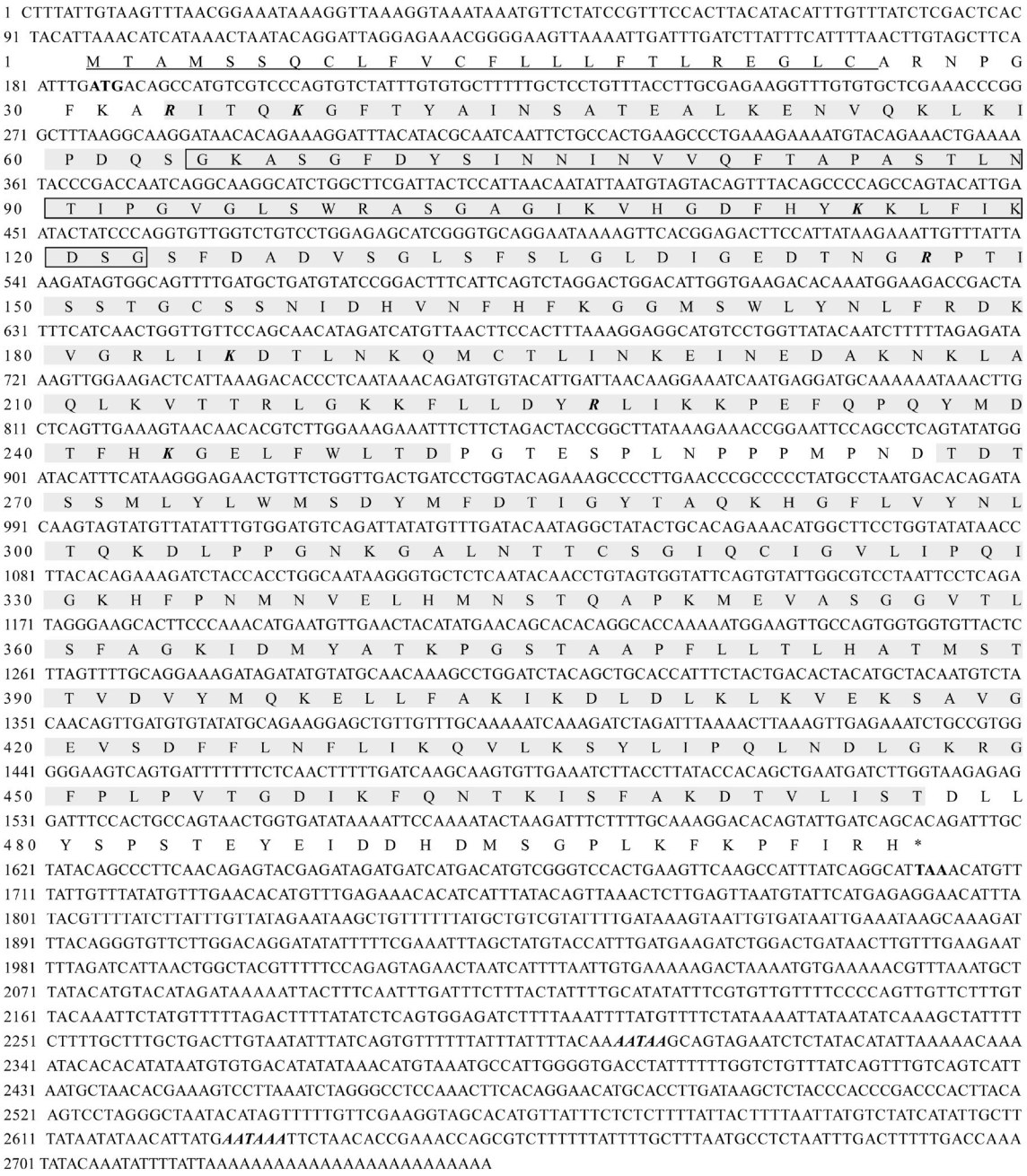

Fig. 1. The complete nucleotide (below) and deduced amino acid (above) sequences of *rpbpi*. The start codon was blacked. The asterisk indicated the stop codon. The predicted signal peptide was underlined. Predicted BPI/LBP/CETP N-terminal and BPI/LBP/CETP C-terminal domain sequences were shown in gray shadow. The LPS-binding domain was boxed. Conserved positions of lysines/arginines (K/R) at the N-terminus and the polyadenylation signal (AATAAA) were indicated by bold italics.

rRpBPI with complete Freund's adjuvant (Sigma, USA) each, and then inoculated with 100 μg rRpBPI with incomplete Freund's adjuvant (Sigma, USA) two weeks later after the first immunization. The third and fourth injections were given by tail vein with 100 μg of rRpBPI at a one-week interval. Seven days after the fourth injection the mice were sacrificed to collect immunized serum [19].

2.8. Western blotting analysis

For western blotting analysis, the rRpBPI protein was separated using 15% SDS-PAGE. Then the separated proteins were electrophoretically transferred onto a nitrocellulose membrane at 300 mA for 90 min. The blotted membrane was blocked with PBS containing 3% bovine serum albumin (BSA) at 4 °C for 12 h and washed three times with PBS containing 0.05% Tween-20 (PBST). After incubated with anti-rRpBPI serum (1:1000 diluted in PBS), the membrane was washed three times with PBST and then incubated with goat-anti-mouse Ig-alkaline phosphatase conjugate (Southern Biotech, 1:5000 diluted in PBS) at 37 °C for 1 h. After the final wash, protein bands were stained with freshly prepared substrate solution NBT/BCIP (Sigma, USA) for 15 min and stopped by rinsing strips with distilled water. Pre-immune serum instead of immunized serum was used as negative control.

2.9. Kinetics of bacterial killing

E. coli, *V. anguillarum and S. aureus* were cultured and harvested at

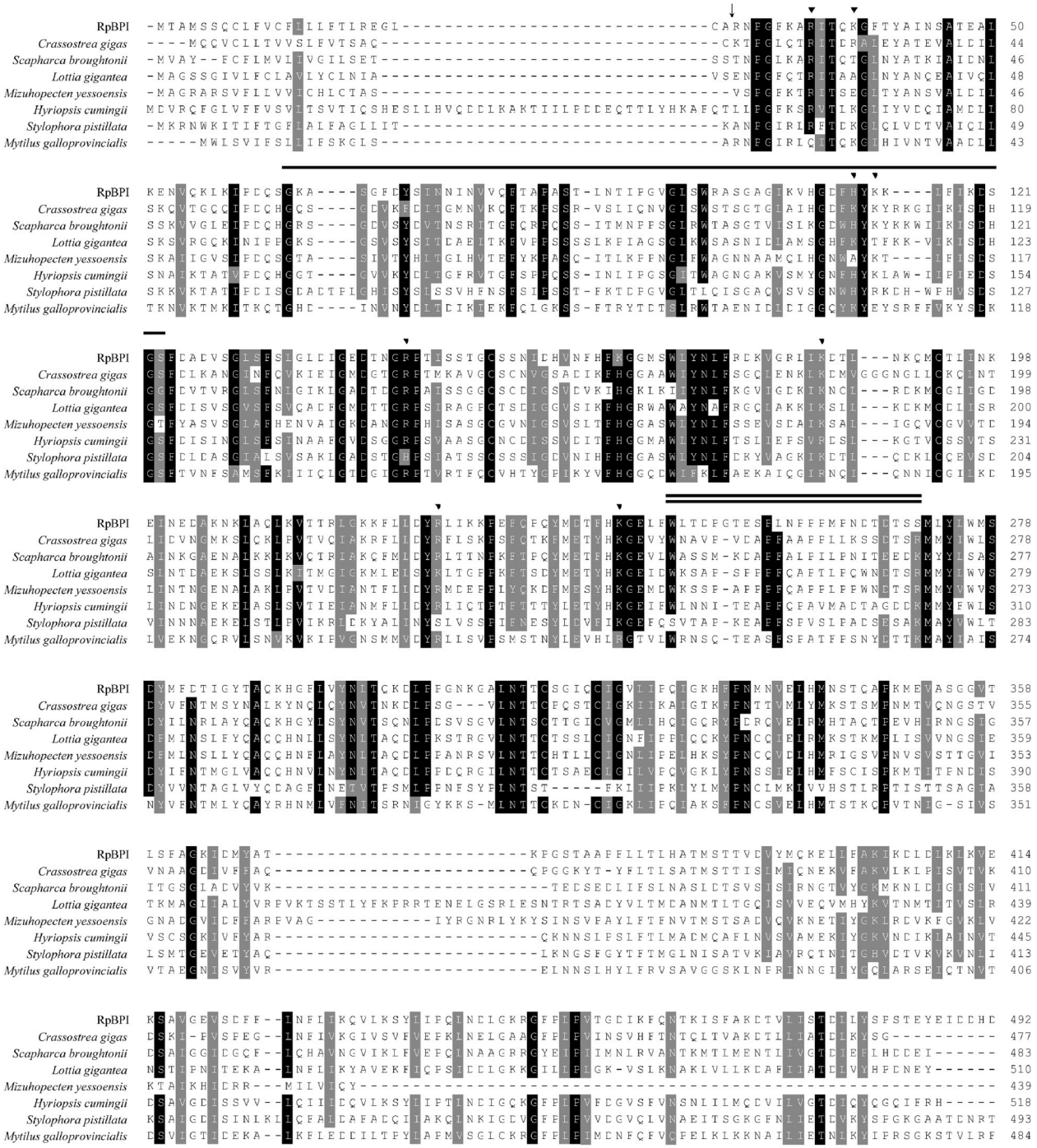

Fig. 2. Multiple alignments of RpBPI with BPIs from other animals, including *Crassostrea gigas* (XP_011451050); *Scapharca broughtonii* (AFQ02695); *Lottia gigantea* (XP_009052399); *Mizuhopecten yessoensis* (XP_021374120); *Hyriopsis cumingii* (ARV86003); *Stylophora pistillata* (PFX21782); *Mytilus galloprovincialis* (AFC37171). Identical residues were marked in dark, and similar amino acids were shaded in gray. An arrow indicated the putative cleavage site by the signal peptidase. The LPS-binding domain and proline-rich domains were labeled by single and double underline, respectively. Conserved lysines/arginines were labeled by triangles (▼).

the logarithmic phase of growth. The bacterial cells were washed twice with sodium phosphate buffer (pH 7.4) and re-suspended to 1.0×10^7 CFU mL^{-1}. The bacterial suspension (100 μL) was incubated with 1.0, 10.0 μM rRpBPI or PBS (control), and the antibacterial activities were measured at 10, 30, 60, 160, 400 and 1000 min at room temperature. The number of surviving bacteria was counted on agar plates and the time-killing curves were plotted with time against the logarithm of the viable count. The results were mean values of at least three independent experiments.

2.10. Biofilm formation

Attached biofilm formation was assayed in 96-well polystyrene plates (Corning Costar, USA) with crystal violet staining [20]. Briefly, *E. coli* MG1655 (OD_{600} = 0.05) was incubated with rRpBPI at concentrations of 0.01 and 0.1 μM for 8 h. Biofilm formation was normalized by dividing the total biofilm by the maximal bacterial growth measured by turbidity at 620 nm. Then the supernatant was poured out, and the plates were washed three times with room temperature water. After the plates were dried, 300 μL 0.1% crystal violet (completely dissolved in

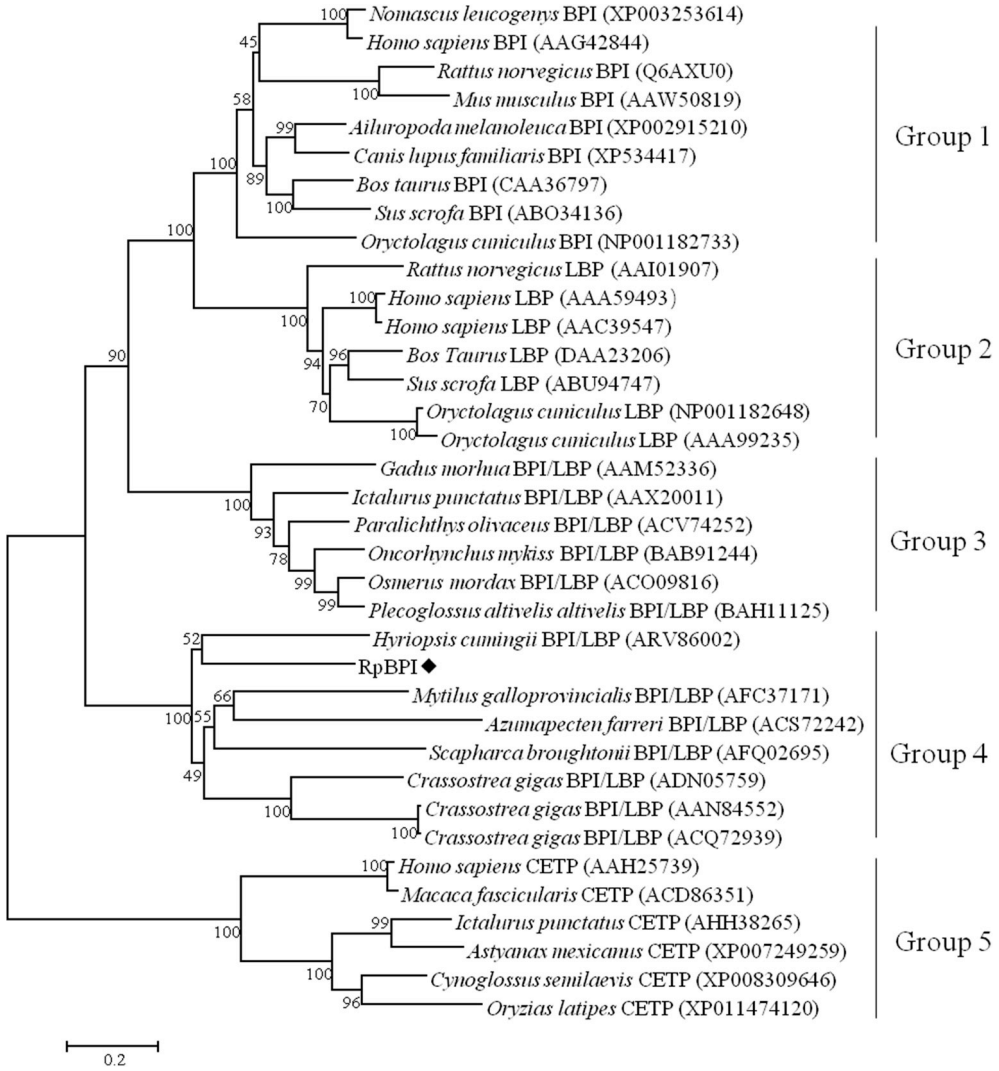

Fig. 3. The neighbor-joining phylogenetic tree of BPI and the other known LBP, BPI, BPI/LBP and CETP proteins from GenBank registered. The number on the nodes represented bootstrap values for 1000 replications. The family of CETP was used as out group.

water solution) was added in each well for 20 min at room temperature. Then the staining solution was poured out, and the plates were washed three times. 300 μL 95% ethanol was added to each well and soaked for 5 min. The total biofilm was measured by turbidity at 540 nm. Ten replicate wells were repeated from two cultures independently.

2.11. PAMPs binding assay

Columns of 96-well assay plate were coated with lipopolysaccharide (LPS), peptidoglycan (PGN), Lipid A or Chitin (Sigma-Aldrich, USA), and blocked with 3% BSA for 12 h as previously described [21]. 100 μL of rRpBPI solution at different concentrations (0.0313, 0.0625, 0.125, 0.25, 0.5 and 1.0 μM) was added to each column and incubated for 3 h at room temperature. After washed three times with PBST, the wells were then incubated with rRpBPI antibody (1:5000) and goat-anti-mouse Ig-alkaline phosphatase conjugate (1:5000) (Southern Biotech, USA). Finally, pNPP substrate solution was added and incubated in dark at room temperature. The absorbance was measured at 405 nm, and the wells with 100 μL of carbonate-bicarbonate buffer were used as blank. Each experiment was carried out in triplicate. The apparent dissociation constant (K_d) values were calculated using Prism 5.00 software (GraphPad software) with a one-site binding model and nonlinear regression analysis, as $A = A_{max}[L]/(K_d + [L])$, where A is the absorbance at 405 nm and [L] is the concentration of the rRpBPI protein.

2.12. Membrane permeability assay

The outer membrane permeability was determined using the 1-N-phenylnaphtylamine (NPN) uptake assay as described previously [22]. Briefly, *E. coli* cells (1×10^7 CFU mL^{-1}) were taken before and after the addition of rRpBPI for 1 h at various concentrations (1.0, 2.5, 5.0, and 10.0 μM). These rRpBPI-treated cells were centrifuged at 5000 rpm for 5 min. After 200 μL NPN (final concentration of 10 μM, acetone) was added, the fluorescence of the samples was measured at an excitation and emission wavelength of 350 and 420 nm with slit widths of 5 nm, respectively. The cells without rRpBPI were served as control.

2.13. Scanning electron microscopy (SEM) analysis

The *V. splendidus* and *V. anguillarum* cells were treated with 1 μM rRpBPI for 1 h and immobilized onto cover glass slides as described previously [23]. Slide-immobilized cells were fixed with 2.5% (w/v) glutaraldehyde in 0.1 M sodium phosphate buffer for 30 min and dehydrated with a graded ethanol series. After critical-point drying and gold coating, the samples were examined by a scanning electron microscope (SEM, Hitachi S-4800, Japan). The negative control was performed in a similar manner with PBS incubation instead of rRpBPI.

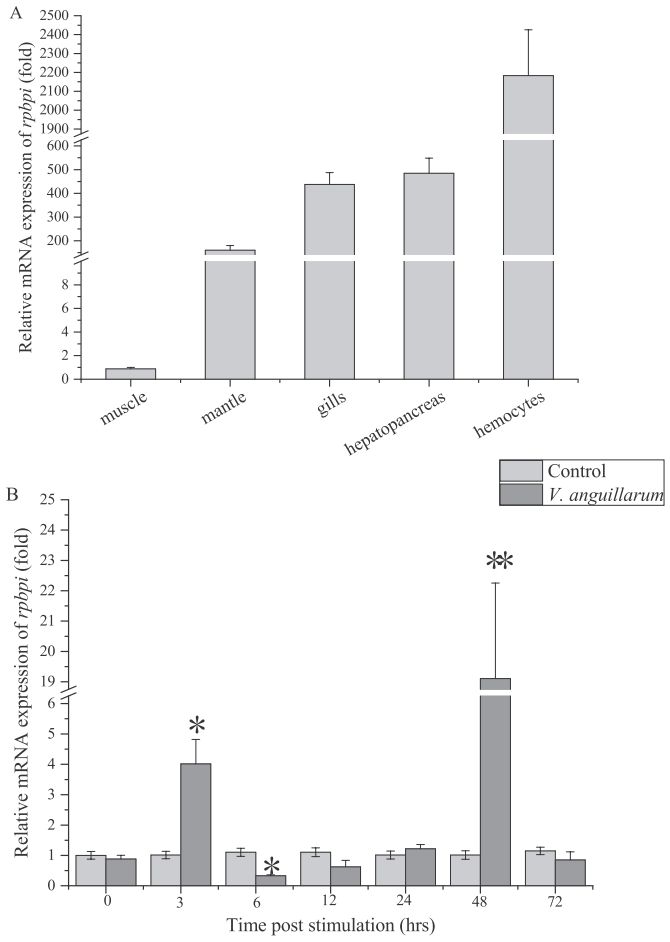

Fig. 4. Tissue distribution (A) and temporal expression (B) of *rpbpi* mRNA detected by qRT-PCR. The values were shown as mean ± S.D. (N = 6) (*: $P < 0.05$, **: $P < 0.01$).

2.14. Phagocytosis assay

Hemolymph was withdrawn from manila clams and mixed immediately with equal volume of pre-chilled anticoagulant buffer (Tris-HCl 50 mM; glucose 2%, NaCl 2%; EDTA 20 mM; pH 7.4). The mixture was centrifuged at 1000 *g* at 4 °C for 10 min to harvest hemocytes. The resultant hemocytes were re-suspended in TBS buffer (Tris-HCl 50 mM; $CaCl_2$ 5 mM) and incubated with rRpBPI (1.0 and 10.0 μM) at 18 °C for 30 min, respectively. Then 5 μL of fluorescent microspheres (5.68×10^9 particles/mL, diameter 2.0 μm, Polyscience, Germany) were added into each hemocytes suspension. The mixture was incubated for 1 h at room temperature, and phagocytosis was then analyzed using an Accuri C6 flow cytometer (BD, USA) with BD CFlow® software. Differences were considered significant at $P < 0.05$ in *t*-test and marked by an asterisk.

3. Results

3.1. Sequence analysis of rpbpi

The full-length cDNA of *rpbpi* was deposited in GenBank database under the accession no. MH559335. The open reading frame (ORF) was of 1518 bp encoding a polypeptide of 505 amino acids with an isoelectric point of 8.8 and predicted molecular weight of 56.1 kDa (Fig. 1). A typical signal peptide of 24 amino acid residues was identified in the N-terminus of *rpbpi* by SignalP software. Blast analysis showed that *rpbpi* exhibited high sequence identities with *bpis* from *Hyriopsis cumingii* (ARV86002, 45% identity) and *Crassostrea gigas* (ACQ72929, 42% identity) (Fig. 2).

A phylogenetic tree was constructed using neighbor-joining method based on *rpbpi* and corresponding sequences from other species. As shown in Fig. 3, the LBPs, BPIs, BPI/LBPs from different species were divided into four different groups with the CETP family used as out group. The BPI/LBP sequences from fish and mollusks segregated into two separate groups. In group 4, the RpBPI clustered together with *H. cumingii*.

3.2. The mRNA distribution of rpbpi in different tissues and temporal expression in response to V. anguillarum challenge

The distribution of *rpbpi* mRNA transcripts in various tissues of uninfected clams was analyzed by qRT-PCR with β-actin as internal control. *rpbpi* transcript was predominantly expressed in hemocytes, moderate in hepatopancreas, gills and mantle, and marginally expressed in adduct muscle (Fig. 4A). The temporal expression of *rpbpi* transcript in hemocytes of clams after bacterial challenge was shown in Fig. 4B. During the first 3 h post pathogen challenge, the expression level of *rpbpi* mRNA was increased up to 4.01-fold of the control group ($P < 0.05$). After that, the expression level was significantly down-regulated at 6 h (0.32-fold, $P < 0.05$). However, the expression of *rpbpi* transcripts reached the maximum at 48 h post challenge, which was 19.10-fold higher than that of the control group ($P < 0.01$). As time progressed, the expression level recovered to the original level at 72 h post challenge.

3.3. Recombinant expression and preparation of rRpBPI antibody

The N-terminal His-tagged fusion peptide rRpBPI was purified using an affinity chromatographic method, and then subjected to SDS-PAGE analysis. A distinct band with molecular weight of about 57 kDa was in agreement with the predicted molecular mass of rRpBPI (Fig. 5A). The concentration and purities of the refolded rRpBPI were approximately 333.7 μg/mL and 96.9% (Fig. 5B), respectively. In western blotting assay, a clear reaction band was revealed (Fig. 5A, line 4), indicating that the antibody could react with rRpBPI with high specificity.

3.4. Antimicrobial activity of rRpBPI

A time-killing experiment was performed with *E. coli*, *V. anguillarum* and *S. aureus* as substrates to investigate the bacteriostatic or bactericidal effects of rRpBPI. As revealed in Fig. 6, a sharp decrease of absorbance was observed in the high concentration group, and both Gram-negative bacteria, but not Gram-positive bacterium were killed within 60 or 160 min, indicating that rRpBPI was perhaps an immune effector mainly against Gram-negative bacteria. Meanwhile, rRpBPI could alter the biofilm formation of *E. coli* MG1655. The incubation of rRpBPI resulted in less biofilm dispersal in a concentration dependent manner (Fig. 7).

3.5. PAMPs binding assay

PAMPs binding assay was performed to detect the binding activity of rRpBPI towards LPS, Lipid A, PGN and Chitin. A dose-dependent binding activity of rRpBPI towards LPS and Lipid A was observed *in vitro* (Fig. 8). The apparent dissociation constant (Kd) of the rRpBPI to LPS and Lipid A was 0.09×10^{-6} M and 0.14×10^{-6} M calculated from the saturation curve fitting according to the one-site specific

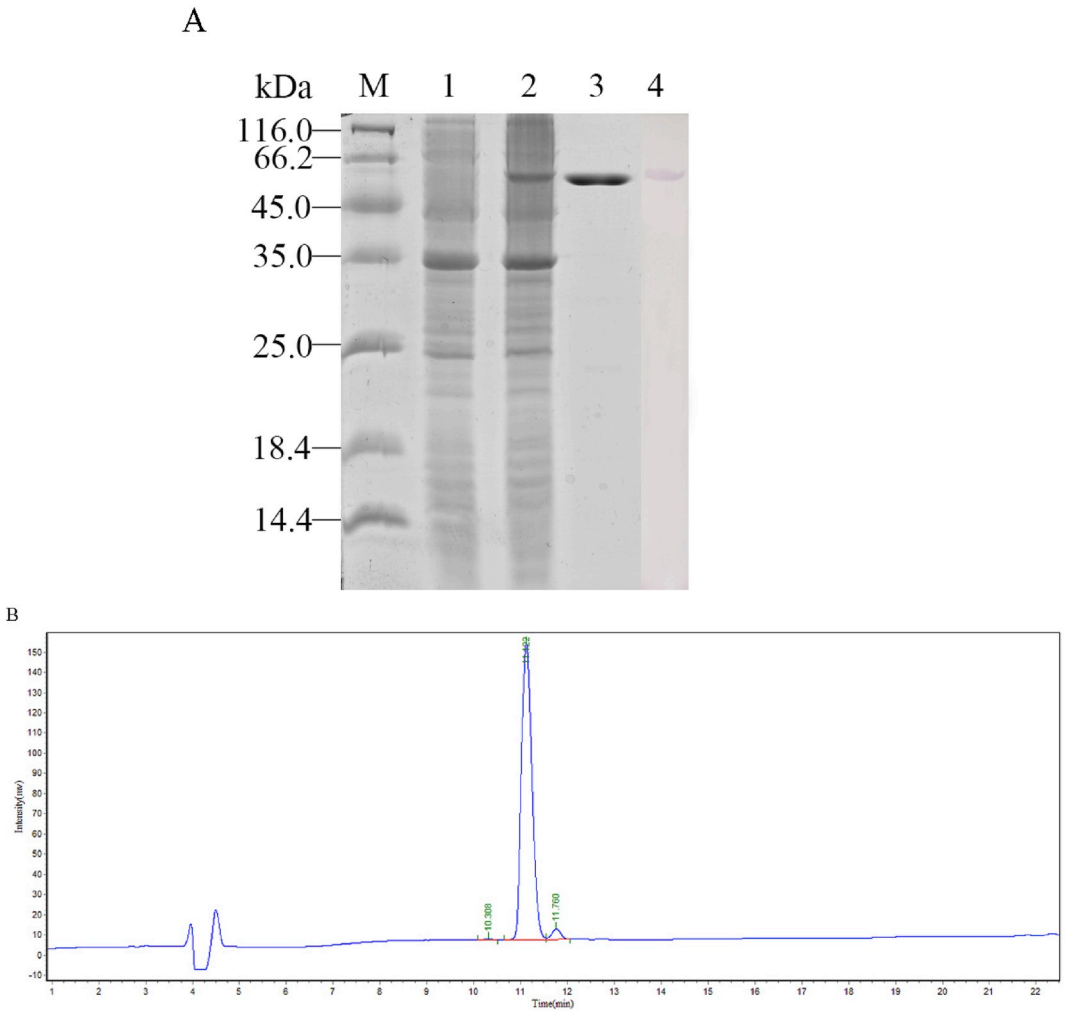

Fig. 5. SDS-PAGE and western-blot analysis of rRpBPI. M: protein marker; lane 1: negative control for rRpBPI (without induction); lane 2: induced rRpBPI; lane 3: purified rRpBPI; lane 4: western blot of rRpBPI.

binding model, respectively (Fig. 8). However, no binding activity of rRpBPI to PGN or Chitin was detected even if at high concentration (data not shown).

3.6. rRpBPI induces the disruption of the membrane integrity

The NPN assay was used to monitor the outer cell membrane permeabilization. As revealed in Fig. 9A, the NPN fluorescence was enhanced to 24.36-fold in 1 μM rRpBPI-treated group compared to the control group. With the increasing of rRpBPI concentration, the NPN fluorescence increased and reached the highest level when incubated with 10 μM rRpBPI (Fig. 9A).

3.7. rRpBPI induces morphological changes of V. Splendidus and V. anguillarum

To further investigate the effect of rRpBPI on bacterial shape, SEM was employed to observe the morphology of *V. splendidus* and *V. anguillarum* in the presence or absence of rRpBPI. After exposed with rRpBPI, bacterial cells showed deep roughening of the cell surface, formation of blebs and contents lost (B and D, Fig. 9B), compared with the smooth surfaces of the untreated group (A and C, Fig. 9B).

3.8. Phagocytosis assay

As revealed in Fig. 10, phagocytosis of the hemocytes could be significantly enhanced by rRpBPI. The phagocytic ability of hemocytes was 21.5% (1.0 μM) and 23.9% (10.0 μM) in the rRpBPI treatment group compared with that of only 15.1% in the control group, respectively.

4. Discussion

Bactericidal/permeability-increasing proteins are important humoral immune factors, and play important roles in the host innate immune responses [24]. Presently, many antibacterial molecules (antimicrobial peptides, lysozymes et al.) have been identified and characterized in marine mollusks. However, the knowledge on the functional characterization of BPI in mollusks is still in its infancy. In the present study, a *bpi* was characterized from manila clams, and the transcriptional responses to pathogen infection, the antibacterial activities and the mode of action were also investigated.

Multiple alignments and phylogenetic analysis revealed that *rpbpi* shared highly similarities with other *bpis* and kept a close evolutionary relationship with *bpis* from other mollusks. An N-terminal BPI/LBP/CETP domain BPI1 and a C-terminal BPI/LBP/CETP domain BPI2 were

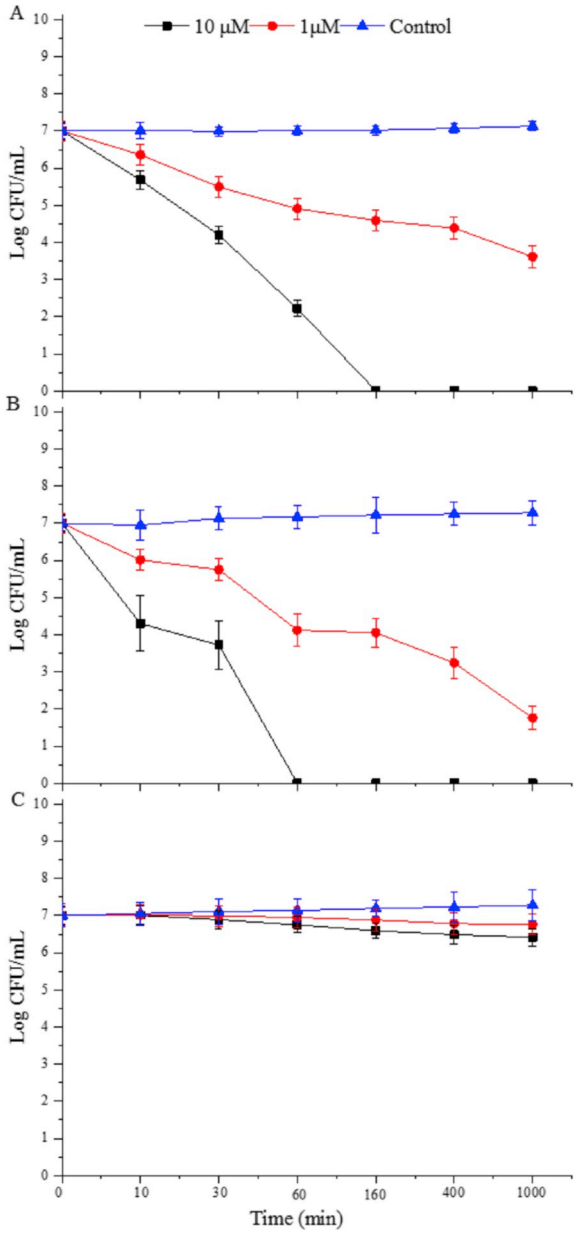

Fig. 6. Bacterial killing kinetics of rRpBPI at 1.0 and 10.0 μM against *E. coli* (A), *V. anguillarum* (B) and *S. aureus* (C). The absorbance was recorded at OD_{450}. Each group had three replicates.

identified in the amino acid sequence of *rpbpi*. It has been reported that the N-terminal BPI1 domain contains three functional regions proposed to be involved in LPS binding, LPS neutralization and bactericidal activity, while the C-terminal BPI2 domain might play roles in mediating LPS binding [11,25]. At the N-terminus, two conserved cysteines involved in the formation of a disulfide bond, were supposed essential for the lipid-binding function between BPI and LPS [26]. Moreover, rich of positively charged amino acid residues (K or R) may facilitate the electrostatic interactions of BPI with the negatively charged groups of LPS [25,27].

Hemocytes play a central role in the mediation of immune capability via phagocytosis, encapsulation and nodule formation [28], and also participate in the processes of tissues/shell repair [29,30] and

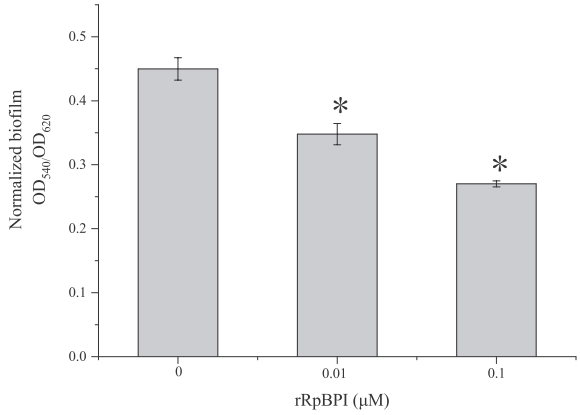

Fig. 7. Biofilm formation of *E. coli* MG1655 treated with rRpBPI. Normalized biofilm formation (total biofilm/growth) was tested in 96-well polystyrene plates after treated with rRpBPI. Data were the average of 10 replicate wells from two independent cultures. The values were shown as mean ± S.D. (N = 10) (*: $P < 0.05$, **: $P < 0.01$).

detoxication [31] in invertebrates. In the present study, the mRNA transcripts of *rpbpi* were dominantly expressed in hemocytes. Notably, phagocytosis of clam hemocytes could be significantly enhanced by rRpBPI. These results support that hemolymph carries immune cells and bioactive molecules (e.g. RpBPI) specialized in pleiotropic defenses against pathogens in manila clams. In other mollusks, the highest constitutive expression of *bpi* transcripts was found in heap hepatopancreases [32] or gills [10]. It was suggested that the specific tissue distribution of different *bpis* could be partially explained by their spatial involvement of microbicidal activities in different tissues of the organisms. Moreover, the transcriptional level of *rpbpi* transcripts in hemocytes was up-regulated significantly post bacterial challenge. It was speculated that during this period, *rpbpi* in hemocytes was processed into active peptide to clear the invaded pathogens, and hemocytes were also mobilized to synthesize *rpbpi* mRNA gradually. As time progresses, drastic increase of *rpbpi* transcript was detected at 48 h primarily due to considerable recruitment of *rpbpi*-producing hemocytes. Considering the moderate killing activity of RpBPI against *V. anguillarum*, the induction levels of *rpbpi* transcript to challenge were relatively high. It was suggested rapid multiply of bacteria might overwhelm the RpBPI in hemolymph and perhaps other AMPs were expected to act synergistically for full activity against this pathogen [32], which was consistent with the fact that *V. anguillarum* is one of the major disease-causing bacteria in manila clam. Similar expression patterns were also reported in other mollusk *bpis*. For example, the expression of *bpi* in hemocytes of ark shell was significantly up-regulated in response to LPS challenge [33].

Many previous studies have found that BPIs from *Apostichopus japonicas* [13] and *Crassostrea gigas* [10] exhibited remarkably antibacterial activities against pathogens. In this study, RpBPI showed antibacterial activities against Gram-negative bacteria. In addition, both *V. anguillarum* and *E. coli* were killed within a few hours after incubated with 10 μM rRpBPI, which supported that BPI was a kind of sterilizing peptide against Gram-negative bacteria. Similarly, all examined Gram-negative bacteria *E. coli* was killed within 3 h after incubated with 1 μM BPI in oyster [11]. Notably, the biofilm formation of *E. coli* was also significantly depressed by rRpBPI even at low concentrations. The limitation on biofilm formation perhaps contributes to the elimination of biofilm-grown bacteria [34]. All these results suggested that RpBPI was involved in the host defense against invasive pathogens.

Many antimicrobial peptides perform antibacterial activities based

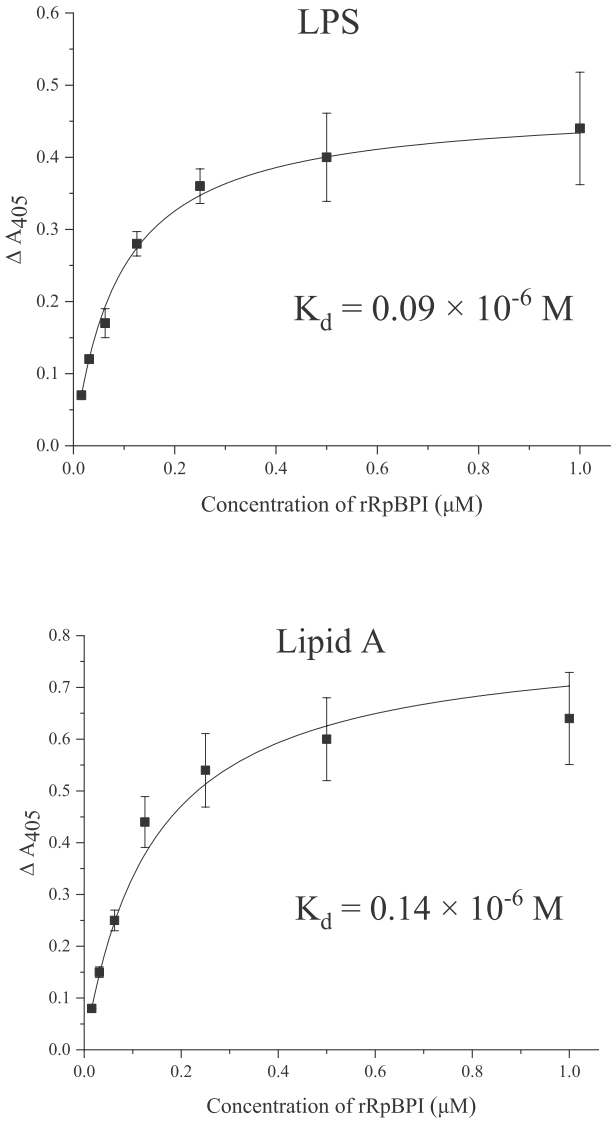

Fig. 8. ELISA assay of the interaction between rRpBPI and the PAMPs. Plates were coated with four kinds of PAMPs including LPS, Lipid A, PGN and chitin, which were washed and incubated with several concentrations of rRpBPI or PBS (data not shown) in the presence of 0.1 mg mL^{-1} BSA at 18 °C for 3 h. After incubated with rRpBPI antibody and goat-anti-mouse Ig-alkaline phosphatase conjugate, the absorbance was recorded at 405 nm. Data are shown as the mean ± 1S.D. (*error bars*) of three individual experiments. The data were curve-fitted using a single-site binding model with $R^2 = 0.94$ for LPS ($K_d = 0.09 \pm 0.005 \times 10^{-6}$ M) and $R^2 = 0.95$ for Lipid A ($K_d = 0.14 \pm 0.01 \times 10^{-6}$ M). Results were representative of the mean of three replicates ± S.D.

on the attraction and attachment to bacterial surface [35]. Usually, three antibacterial mechanisms were widely accepted, such as membrane dysfunction (pore forming), inhibition of extracellular biopolymer synthesis or intracellular functions [11]. In the present study, rRpBPI could bind to LPS and Lipid A in a concentration-dependent manner. Consistent with the results in oyster, Cg-BPI perform strong affinity to LPS and Lipid A and then disrupted the bacterial cytoplasmic membrane [36,37]. The high antibacterial activity of rRpBPI against *E. coli* may lie in the high binding activity to LPS or Lipid A. In addition, NPN assay and SEM analysis revealed that rRpBPI induced a remarkable modification of cell membrane. Thus, our results supported that rRpBPI might kill bacteria by destroying the bacterial membrane.

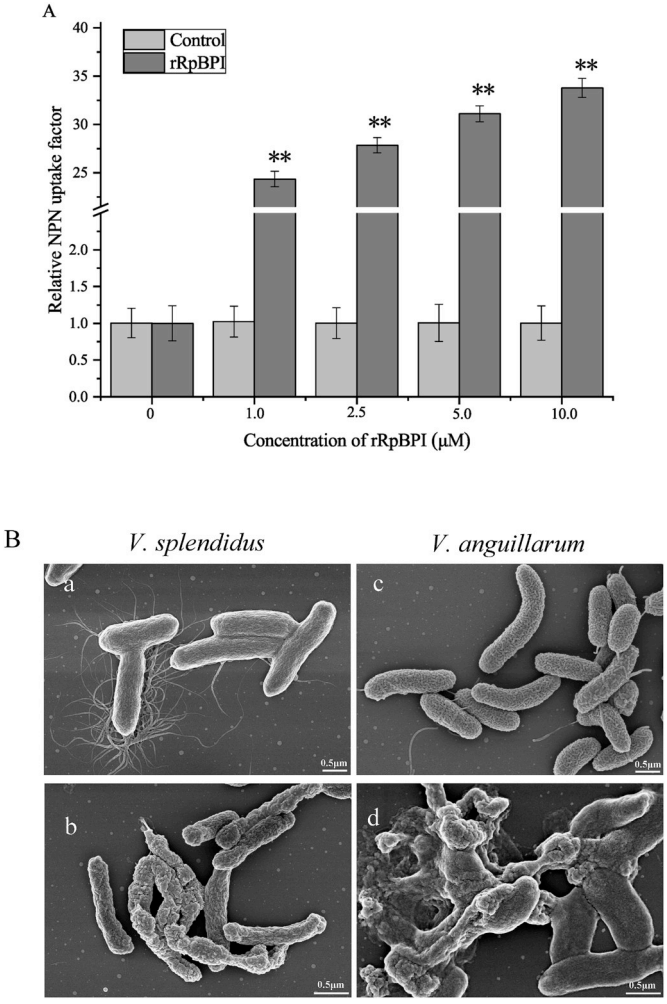

Fig. 9. Outer membrane permeabilization of *E. coli* (A). Permeabilization of the outer membrane was monitored as an increase in NPN fluorescence intensity in the presence of rRpBPI (1.0 μM). Each group had three replicates. SEM images of *V. splendidus* and *V. anguillarum* in the absence (a, c) or presence (b, d) of rRpBPI (1.0 μM) after exposure for 1 h (B).

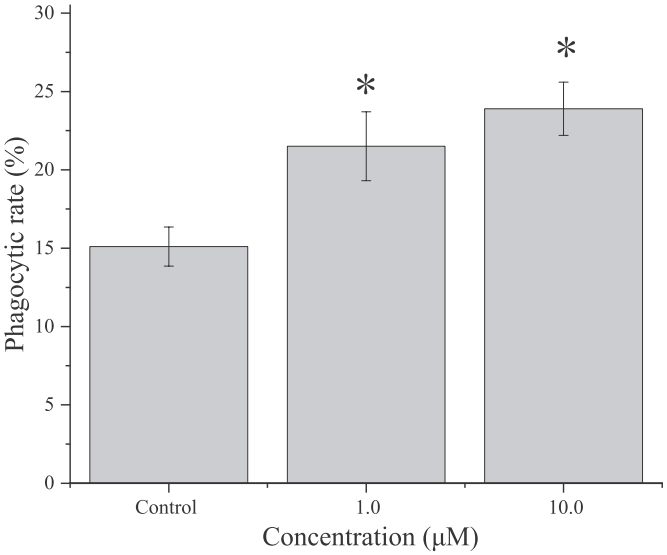

Fig. 10. Phagocytosis of hemocytes enhanced by rRpBPI. Phagocytosis was analyzed using an Accuri C6 flow cytometer (BD) with BD CFlow® software. The values were shown as mean ± S.D. (N = 3) (*: $P < 0.05$, **: $P < 0.01$).

Acknowledgements

This research was supported by grants from the Strategic Priority Research Program of the Chinese Academy of Sciences (XDA23050303), the National Natural Science Foundation of China (No. 41806196), Key Research Program of the Chinese Academy of Sciences (No. KZZD-EW-14 and KFJ-STS-ZDTP-023), Two-Hundred Talents Plan of Yantai (Y839081021), Natural Science Foundation of Shandong Province (ZR2019BD022) and the Youth Innovation Promotion Association, CAS (2016196).

Appendix A. Supplementary data

Supplementary data to this article can be found online at https://doi.org/10.1016/j.fsi.2019.08.050.

References

[1] B.H. Nam, K.J. Ahn, Y.O. Kim, H.J. Kong, W.J. Kim, H.S. Kim, S.J. Lee, K.K. Kim, Molecular cloning and characterization of LPS-binding protein/bactericidal permeability-increasing protein (LBP/BPI) from olive flounder, *Paralichthys olivaceus*, Vet. Immunol. Immunopathol. 133 (2–4) (2010) 256–263.

[2] C.J. Kirschning, J. Au-Young, N. Lamping, D. Reuter, D. Pfeil, J.J. Seilhamer, R.R. Schumann, Similar organization of the lipopolysaccharide-binding protein (LBP) and phospholipid transfer protein (PLTP) genes suggests a common gene family of lipid-binding proteins, Genomics 46 (3) (1997) 416–425.

[3] R.R. Schumann, S.R. Leong, G.W. Flaggs, P.W. Gray, S.D. Wright, J.C. Mathison, P.S. Tobias, R.J. Ulevitch, Structure and function of lipopolysaccharide binding-protein, Science 249 (4975) (1990) 1429–1431.

[4] R.J. Ulevitch, P.S. Tobias, Receptor-dependent mechanisms of cell stimulation by bacterial-endotoxin, Annu. Rev. Immunol. 13 (1995) 437–457.

[5] P. Elsbach, J. Weiss, The bactericidal permeability-increasing protein (Bpi), a potent element in host-defense against Gram-negative bacteria and lipopolysaccharide, Immunobiology 187 (3–5) (1993) 417–429.

[6] H. Inagawa, T. Honda, C. Kohchi, T. Nishizawa, Y. Yoshiura, T. Nakanishi, Y. Yokomizo, G.I. Soma, Cloning and characterization of the homolog of mammalian lipopolysaccharide-binding protein and bactericidal permeability-increasing protein in rainbow trout *Oncorhynchus mykiss*, J. Immunol. 168 (11) (2002) 5638–5644.

[7] O. Levy, R.B. Sisson, J. Kenyon, E. Eichenwald, A.B. Macone, D. Goldmann, Enhancement of neonatal innate defense: effects of adding an N-terminal recombinant fragment of bactericidal/permeability-increasing protein on growth and tumor necrosis factor-inducing activity of gram-negative bacteria tested in neonatal cord blood *ex vivo*, Infect. Immun. 68 (9) (2000) 5120–5125.

[8] P.H. Reichel, C. Seemann, E. Csernok, J.M. Schroder, A. Muller, W.L. Gross, H. Schultz, Bactericidal/permeability-increasing protein is expressed by human dermal fibroblasts and upregulated by interleukin 4, Clin. Diagn. Lab. Immunol. 10 (3) (2003) 473–475.

[9] J. Weiss, P. Elsbach, I. Olsson, H. Odeberg, Purification and characterization of a potent bactericidal and membrane active protein from granules of human polymorphonuclear leukocytes, J. Biol. Chem. 253 (8) (1978) 2664–2672.

[10] Y. Zhang, X.C. He, X.M. Li, D.K. Fu, J.H. Chen, Z.N. Yu, The second bactericidal permeability increasing protein (BPI) and its revelation of the gene duplication in the Pacific oyster, *Crassostrea gigas*, Fish Shellfish Immunol. 30 (3) (2011) 954–963.

[11] M. Gonzalez, Y. Gueguen, D. Destoumieux-Garzon, B. Romestand, J. Fievet, M. Pugniere, F. Roquet, J.M. Escoubas, F. Vandenbulcke, O. Levy, L. Saune, P. Bulet, E. Bachere, Evidence of a bactericidal permeability increasing protein in an invertebrate, the *Crassostrea gigas* Cg-BPI, P Natl Acad Sci USA 104 (45) (2007) 17759–17764.

[12] B. Allam, C. Paillard, S.E. Ford, Pathogenicity of *Vibrio tapetis*, the etiological agent of brown ring disease in clams, Dis. Aquat. Org. 48 (3) (2002) 221–231.

[13] Y.N. Shao, C.H. Li, Z.J. Che, P.J. Zhang, W.W. Zhang, X.M. Duan, Y. Li, Cloning and characterization of two lipopolysaccharide-binding protein/bactericidal permeability-increasing protein (LBP/BPI) genes from the sea cucumber *Apostichopus japonicus* with diversified function in modulating ROS production, Dev. Comp. Immunol. 52 (1) (2015) 88–97.

[14] J.J.M. Hathaway, C.M. Adema, B.A. Stout, C.D. Mobarak, E.S. Loker, Identification of protein components of egg masses indicates parental investment in immunoprotection of offspring by *Biomphalaria glabrata* (Gastropoda, Mollusca), Dev. Comp. Immunol. 34 (4) (2010) 425–435.

[15] J.M. Zhao, C.H. Li, A.Q. Chen, L.Y. Li, X.R. Su, T.W. Li, Molecular characterization of a novel big defensin from clam *Venerupis philippinarum*, PLoS One 5 (10) (2010).

[16] J. Schultz, F. Milpetz, P. Bork, C.P. Ponting, SMART, a simple modular architecture research tool: Identification of signaling domains, P Natl Acad Sci USA 95 (11) (1998) 5857–5864.

[17] K.J. Livak, T.D. Schmittgen, Analysis of relative gene expression data using real-time quantitative PCR and the 2(T)(-Delta Delta C) method, Methods 25 (4) (2001) 402–408.

[18] Q. Wang, C.Y. Wang, C.K. Mu, H.F. Wu, L.B. Zhang, J.M. Zhao, A novel c-type lysozyme from *Mytilus galloprovincialis*: insight into innate immunity and molecular evolution of invertebrate c-type lysozymes, PLoS One 8 (6) (2013).

[19] S. Cheng, W. Zhan, J. Xing, X. Sheng, Development and characterization of monoclonal antibody to the lymphocystis disease virus of Japanese flounder *Paralichthys olivaceus* isolated from China, J. Virol. Methods 135 (2) (2006) 173–180.

[20] L.A. Pratt, R. Kolter, Genetic analysis of *Escherichia coli* biofilm formation: roles of flagella, motility, chemotaxis and type I pili, Mol. Microbiol. 30 (2) (1998) 285–293.

[21] P.S. Yan, T. Efferth, H.L. Chen, J. Lin, F. Rodel, L. Fuzesi, T.H.M. Huang, Use of CpG island microarrays to identify colorectal tumors with a high degree of concurrent methylation, Methods 27 (2) (2002) 162–169.

[22] D. Nievagomez, J. Konisky, R.B. Gennis, Membrane Changes in *Escherichia coli* induced by colicin ia and agents known to disrupt energy transduction, Biochemistry-Us 15 (13) (1976) 2747–2753.

[23] L.B. Zhang, D.L. Yang, Q. Wang, Z.Y. Yuan, H.F. Wu, D. Pei, M. Cong, F. Li, C.L. Ji, J.M. Zhao, A defensin from clam *Venerupis philippinarum*: molecular characterization, localization, antibacterial activity, and mechanism of action, Dev. Comp. Immunol. 51 (1) (2015) 29–38.

[24] J.A. Tincu, S.W. Taylor, Antimicrobial peptides from marine invertebrates, Antimicrob. Agents Chemother. 48 (10) (2004) 3645–3654.

[25] N. Lamping, A. Hoess, B. Yu, T.C. Park, C.J. Kirschning, D. Pfeil, D. Reuter, S.D. Wright, F. Herrmann, R.R. Schumann, Effects of site-directed mutagenesis of basic residues (Arg 94, Lys 95, Lys 99) of lipopolysaccharide (LPS)-binding protein on binding and transfer of LPS and subsequent immune cell activation, J. Immunol. 157 (10) (1996) 4648–4656.

[26] A.H. Horwitz, S.D. Leigh, S. Abrahamson, H. GazzanoSantoro, P.S. Liu, R.E. Williams, S.F. Carroll, G. Theofan, Expression and characterization of cysteine-modified variants of an amino-terminal fragment of bactericidal/permeability-increasing protein, Protein Expr. Purif. 8 (1) (1996) 28–40.

[27] L.J. Beamer, S.F. Carroll, D. Eisenberg, The BPI/LBP family of proteins: a structural analysis of conserved regions, Protein Sci. 7 (4) (1998) 906–914.

[28] V. Matozzo, L. Ballarin, D.M. Pampanin, M.G. Marin, Effects of copper and cadmium exposure on functional responses of hemocytes in the clam, *Tapes philippinarum*, Arch Environ Con Tox 41 (2) (2001) 163–170.

[29] T. Suzuki, R. Yoshinaka, S. Mizuta, S. Funakoshi, K. Wada, Extracellular-matrix formation by amebocytes during epithelial regeneration in the pearl oyster *Pinctada-fucata*, Cell Tissue Res. 266 (1) (1991) 75–82.

[30] A.S. Mount, A.P. Wheeler, R.P. Paradkar, D. Snider, Hemocyte-mediated shell mineralization in the eastern oyster, Science 304 (5668) (2004) 297–300.

[31] L. Giamberini, M. Auffret, J.C. Pihan, Haemocytes of the freshwater mussel, Dreissena polymorpha pallas: cytology, cytochemistry and X-ray microanalysis, J. Molluscan Stud. 62 (1996) 367–379.

[32] P. Jena, B. Mishra, M. Leippe, A. Hasilik, G. Griffiths, A. Sonawane, Membrane-active antimicrobial peptides and human placental lysosomal extracts are highly active against mycobacteria, Peptides 32 (5) (2011) 881–887.

[33] Y.Z. Mao, C.Y. Zhou, L. Zhu, Y. Huang, T.R. Yan, J.G. Fang, W. Zhu, Identification and expression analysis on bactericidal permeability-increasing protein (BPI)/lipopolysaccharide-binding protein (LBP) of ark shell, *Scapharca broughtonii*, Fish Shellfish Immunol. 35 (3) (2013) 642–652.

[34] S.C. Park, Y. Park, K.S. Hahm, The Role of antimicrobial peptides in preventing multidrug-resistant bacterial infections and biofilm formation, Int. J. Mol. Sci. 12 (9) (2011) 5971–5992.

[35] S.V. Sperstad, T. Haug, H.M. Blencke, O.B. Styrvold, C. Li, K. Stensvag, Antimicrobial peptides from marine invertebrates: challenges and perspectives in marine antimicrobial peptide discovery, Biotechnol. Adv. 29 (5) (2011) 519–530.

[36] M.R. Yeaman, N.Y. Yount, Mechanisms of antimicrobial peptide action and resistance, Pharmacol. Rev. 55 (1) (2003) 27–55.

[37] Y. Shai, Mode of action of membrane active antimicrobial peptides, Biopolymers 66 (4) (2002) 236–248.